

Artificial Intelligence–Based Diagnostic Model for Detecting Keratoconus Using Videos of Corneal Force Deformation

Zuoping Tan^{1,*}, Xuan Chen^{2,*}, Kangsheng Li³, Yan Liu³, Huazheng Cao², Jing Li⁴, Vishal Jhanji⁵, Haohan Zou², Fenglian Liu³, Riwei Wang¹, and Yan Wang^{2,6} 

¹ Wenzhou University of Technology, Wenzhou, Zhejiang, China

² Clinical College of Ophthalmology, Tianjin Medical University, Tianjin, China

³ Tianjin University of Technology, Tianjin, China

⁴ Shanxi Eye Hospital, Xi'an People's Hospital, Xi'an, Shanxi, China

⁵ Department of Ophthalmology, University of Pittsburgh School of Medicine, Pittsburgh, PA, USA

⁶ Tianjin Eye Hospital, Tianjin Eye Institute, Tianjin Key Laboratory of Ophthalmology and Visual Science, Nankai University Affiliated Eye Hospital, Tianjin, China

Correspondence: Yan Wang, Clinical College of Ophthalmology, Tianjin Medical University, Tianjin Eye Hospital, Tianjin Eye Institute, Tianjin Key Laboratory of Ophthalmology and Visual Science, Nankai University Affiliated Eye Hospital, No 4. Gansu Road, He-ping District, Tianjin 300020, China.

e-mail: wangyan7143@vip.sina.com

Riwei Wang, Wenzhou University of Technology, No. 1 Landscape Avenue, Chashan Street, Ouhai District, Wenzhou 325035, Zhejiang, China.

e-mail: wangrw@wzu.edu.cn

Received: April 2, 2022

Accepted: August 22, 2022

Published: September 30, 2022

Keywords: keratoconus; artificial intelligence; dynamic videos; corneal biomechanics

Citation: Tan Z, Chen X, Li K, Liu Y, Cao H, Li J, Jhanji V, Zou H, Liu F, Wang R, Wang Y. Artificial intelligence–based diagnostic model for detecting keratoconus using videos of corneal force deformation. *Transl Vis Sci Technol.* 2022;11(9):32, <https://doi.org/10.1167/tvst.11.9.32>

Purpose: To develop a novel method based on biomechanical parameters calculated from raw corneal dynamic deformation videos to quickly and accurately diagnose keratoconus using machine learning.

Methods: The keratoconus group was included according to Rabinowitz's criteria, and the normal group included corneal refractive surgery candidates. Independent biomechanical parameters were calculated from dynamic corneal deformation videos. A novel neural network model was trained to diagnose keratoconus. Tenfold cross-validation was performed, and the sample set was divided into a training set for training, a validation set for parameter validation, and a testing set for performance evaluation. External validation was performed to evaluate the model's generalizability.

Results: A novel intelligent diagnostic model for keratoconus based on a five-layer feedforward network was constructed by calculating four biomechanical characteristics, including time of the first applanation, deformation amplitude at the highest concavity, central corneal thickness, and radius at the highest concavity. The model was able to diagnose keratoconus with 99.6% accuracy, 99.3% sensitivity, 100% specificity, and 100% precision in the sample set ($n = 276$), and it achieved an accuracy of 98.7%, sensitivity of 97.4%, specificity of 100%, and precision of 100% in the external validation set ($n = 78$).

Conclusions: In the absence of corneal topographic examination, rapid and accurate diagnosis of keratoconus is possible with the aid of machine learning. Our study provides a new potential approach and sheds light on the diagnosis of keratoconus from a purely corneal biomechanical perspective.

Translational Relevance: Our findings could help improve the diagnosis of keratoconus based on corneal biomechanical properties.

Introduction

Keratoconus (KC) is characterized by central and paracentral corneal thinning that leads to irregular astigmatism, causing deterioration of visual acuity and even loss of vision, with negative consequences on the quality of life.¹ The etiology of KC is not fully understood. Genetics, collagen disorders, endocrine and cellular metabolism, allergies, and immune deficiencies may be involved in its occurrence.² KC is an absolute contraindication for corneal refractive surgery. The risk of corneal ectasia increases after refractive surgery, probably because surgical ablation of the cornea stimulates the progression of occult KC.³ Therefore, the accurate identification of KC is necessary during preoperative screening for corneal refractive surgery.

Machine learning (ML) can model the learning behavior of humans and continuously refine its own performance to specific requirements. ML is gaining increasing attention in many fields of medicine,⁴ including ophthalmology.⁵ It has been applied in KC detection,⁶ as well as in the analysis of corneal images.⁷⁻⁹ Recently, the concepts of corneal biomechanics have been employed for KC detection. Changes in biomechanical properties may precede alterations in corneal morphology in KC.¹⁰ Therefore, focusing on corneal biomechanics may be valuable in the diagnosis of KC.

Previous studies on ML were based solely on static images or specific parameters generated from devices without considering the potential influence of correlation between parameters on the diagnostic model, thereby limiting the reliability of the diagnosis.¹¹⁻¹³ Moreover, previous studies have found correlations only between KC and certain biomechanical indices, and to date, no diagnostic model has been found to directly diagnose KC based on corneal biomechanical alterations.^{14,15} The current study, with the aid of ML approaches, attempts to analyze the corneal dynamic deformation process to diagnose KC solely from a corneal biomechanical perspective.

Methods

Participants

A total of 177 KC eyes of 143 participants were examined in the Refractive Surgery Centre at the Tianjin Eye Hospital (Tianjin Medical University, Tianjin, China). A total of 177 normal eyes of 118 participants were enrolled over the same period. All participants underwent routine ophthalmic examinations and provided informed consent after an expla-

nation of the nature and possible consequences of the study. This study was approved by the China Clinical Trial Centre (ChiCTR2000037484) and the Ethics Review Committee of Tianjin Ophthalmic Hospital (2021025). All study procedures followed the tenets of the Declaration of Helsinki.

Inclusion and Exclusion Criteria

KC was defined by the presence of one of the following clinical signs: stromal thinning, Fleischer's ring, Vogt's striae, Munson's sign, epithelial or subepithelial scarring associated with a typical topographic pattern (asymmetric bow tie with a skewed radial axis), central K-value >47.00 diopters (D) and inferior-superior asymmetry (I-S value) >3.0 D according to Rabinowitz's criteria,¹ and a corrected distance visual acuity <1.0 . All participants had no history of wearing contact lenses.

The inclusion criteria for the control group were as follows: randomly selected candidates for corneal refractive surgery with no history of ocular surgery or trauma, no active ocular disease, and a corrected distance visual acuity ≥ 1.0 . Contact lenses were discontinued (soft contact lenses for at least 2 weeks, rigid contact lenses for at least 4 weeks, and keratoplasty lenses for at least 3 months) before corneal assessments.

Data Acquisition

Demographic data, such as participants' age and gender, were recorded, and visual acuity, as well as objective and manifest refraction, was measured. Additionally, slit-lamp microscopy, noncontact intraocular pressure, funduscopy, corneal morphology, and corneal biomechanics were performed.

Corneal biomechanics of all participants were measured using Corvis ST (Corneal Visualization Scheimpflug Technology; Oculus, Wetzlar, Germany). Corvis ST applanates the cornea using a puff of air, and the corneal deformation process is recorded by a Scheimpflug high-speed camera at a shot speed of 4330 frames/s. During the examination, the participant was seated in a stable position on a chinrest. They were then asked to blink and then look at a fixed point to expose the cornea. The examiner next adjusted the joystick, and the machine automatically identified the cornea and applied pressure by spraying pulsed air to obtain dynamic corneal response parameters, waveforms, and videos. During the measurements, air pulse application of pressure onto the corneal surface caused deformation, with downward depression reaching first, then flattening, and then reaching the highest concavity. This was immediately followed by a second

flattening during the recovery process of deformation and then a return to a natural state after brief fluctuations. Measurements were recorded only when the “Quality Control Score” displayed “OK.”

Learning Model

This study used a video that records the entire dynamic process of the cornea undergoing deformation by force to calculate the parameters by which the cornea is subjected to air pulses that reflect its biomechanical properties.

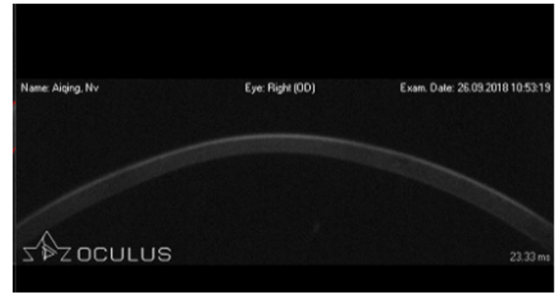
The first step was to sample and analyze the video, which had a total time of 31.88 ms and 139 total frames. Every 0.23 ms ($31.88 \text{ ms}/139 = 0.23 \text{ ms}$), a frame was obtained, and a total of 115,200 corneal contour data points were extracted from each frame’s data on the corneal contour. An image from the video is shown in Figure 1. We used the least squares method to fit a straight line near the corneal apex and calculated the time to the first appplanation. We obtained HC-DA by calculating the distance between the initial position of the corneal apex and the nadir at the highest concavity. We used the curvature formula to calculate the radius of curvature at the maximum concavity, HC-R. In the normal state, the distance between the anterior and the posterior surface is the central corneal thickness (CCT). We then used the four corneal biomechanical parameters calculated above to train the feedforward neural network model, 5-FNN, to distinguish normal corneas from KC.

The 5-FNN model is based on error backpropagation and is a parallel-distributed network with three hidden layers containing 20 neurons each. This enhances the expressiveness of the model and makes it suitable for KC diagnosis. It is a supervised learning algorithm that completes predictions through forward propagation and training by backpropagation.

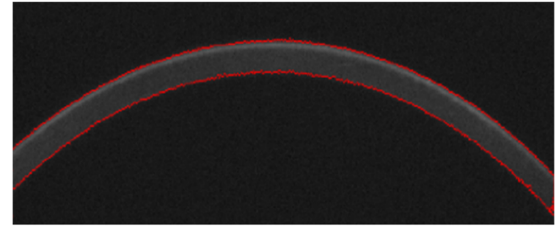
This study trained a 5-FNN model with 276 samples (half with keratoconus and half with normal corneas) to find the appropriate coefficient matrix W^l and offset b^l to construct a predictive model for KC. We used the mean squared error as the loss function to measure the output loss of the training samples; that is, we expected to minimize the following equation:

$$\begin{aligned} \min_{W,b} J(W, b, x, y) &= \frac{1}{2} \|a^l - y\|_2^2 \\ &= \frac{1}{2} \|\sigma(W^l a^{l-1} + b^l) - y\|_2^2. \end{aligned}$$

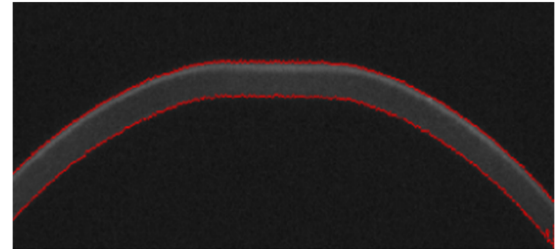
We used the gradient descent method to iteratively solve each layer for W^l and b^l .



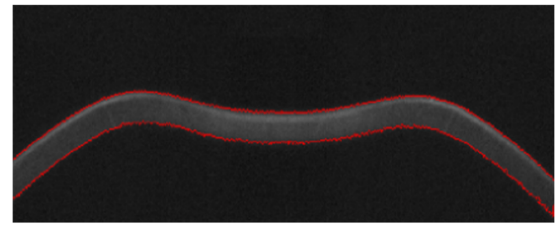
Corneal raw video



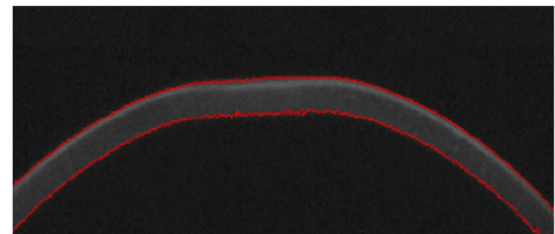
Initial corneal contour



First appplanation



Highest concavity



Second appplanation

Figure 1. Corneal contour data. Corneal force deformation processes recorded with Corvis ST. By segmenting the dynamic video, the original corneal contour is extracted, and corneal biomechanical parameters are calculated.

Statistical Analysis

Tenfold cross-validation was performed. The sample set was divided into 10 mutually exclusive subsets, and each subset had a similar distribution. Nine subsets were used to develop the parameters (eight subsets composed the training set and were used for training while one subset composed the validation set and was used for parameter validation); the remaining subset was used as the test set to evaluate performance. This process was randomly repeated 10 times, and the average value was used as the final result. Moreover, an external validation set was used to validate the model's generalizability.

We defined the evaluation criteria for classifying concordant and discordant results as follows:

- TP (true positive): Number of correctly classified KC

- FP (false positive): Number of normal eyes misclassified as KC
- TN (true negative): Number of correctly classified normal eyes
- FN (false negative): Number of KC misclassified as normal eyes

For each 10 repetitions, the accuracy, sensitivity, specificity, and precision were calculated as follows:

- Accuracy = $(TP + TN) / (TP + FP + TN + FN)$
- Sensitivity = $TP / (TP + FN)$
- Specificity = $TN / (TN + FP)$
- Precision = $TP / (TP + FP)$

All statistical analyses were performed using Statistical Package for the Social Sciences version 26.0 software (International Business Machines Corp., Armonk, NY, USA). Receiver operating characteristic

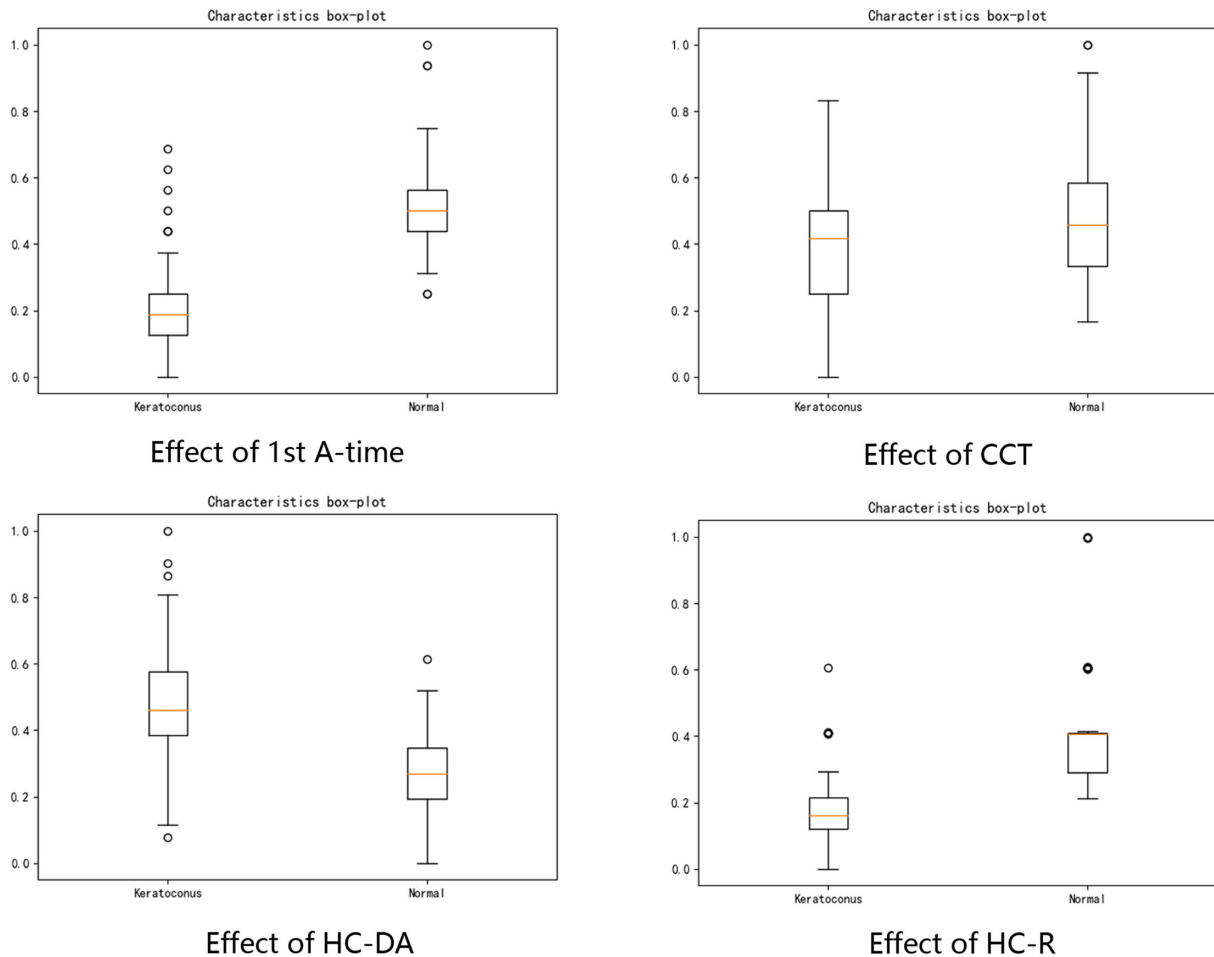


Figure 2. Visual analysis of the role of the parameters. Distribution of parameter values visualized to analyze differences between keratoconus and normal corneas. 1st A-time, the first appplanation time; HC-DA, highest concavity deformation amplitude; HCR, highest concavity radius.

curve was used to analyze the ability of Corvis Biomechanical Index (CBI) to diagnose keratoconus and to calculate the cutoff value for the best diagnostic ability.

Results

A total of 177 KC eyes of 143 patients (93 men and 50 women; age range, 14–40 years; median age, 23.96 ± 5.02 years) and 177 normal eyes of 118 participants (66 men and 52 women; age range, 18–43 years; median age, 24.42 ± 5.93 years) were included in this study; 354 corneal dynamic deformation videos (half with keratoconus and half with normal corneas) were analyzed, of which 276 were for training and testing and 78 were for external validation. The first A-time, HC-DA, CCT, and HC-R were calculated after extracting corneal contours using the OTSU algorithm incorporating logistics with morphology, which were then used for constructing the 5-FNN model.

We calculated the first A-time, HC-DA, CCT, and HC-R on pixel-level data and then used these four corneal biomechanical parameters to train the 5-FNN model to distinguish normal corneas from KC without corneal morphologic examination or clinical signs and symptoms. The four corneal biomechanical characteristics used in our 5-FNN model could effectively distinguish KC from normal eyes, and the effects of the four corneal biomechanical parameters on KC occurrence were further investigated by visual analysis, as shown in Figure 2. There were significant differences in first A-time, HC-DA, and HC-R between KC and normal corneas.

We calculated novel neural network model predictions using the standard statistics as described in the methods, where 138 normal eyes were correctly classi-

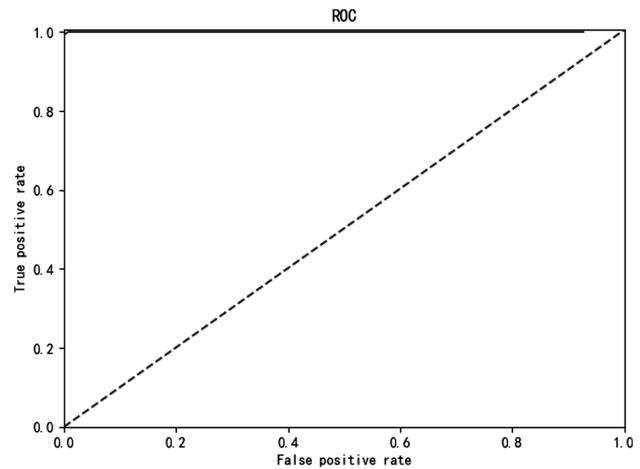


Figure 3. Receiver operating characteristic curve.

fied as normal, and 137 KC were correctly classified as KC. Of the latter, one case of KC was misclassified as a normal eye in the sample set. A comparison of the different biomechanical properties is presented in Table 1.

In the sample set ($n = 276$), we used CBI to separate normal from keratoconic eyes, with a cutoff value of 0.329, with 96.4% accuracy, 92.7% sensitivity, 100% specificity, and 100% precision. We found that our 5-FNN model could detect KC with 99.6% accuracy, 99.3% sensitivity, 100% specificity, and 100% precision compared to support vector machine and computer-aided diagnosis (Table 2). The receiver operating characteristic curve is shown in Figure 3. In the external validation set ($n = 78$), the accuracy for the diagnosis of keratoconus was 98.7%, sensitivity was 97.4%, specificity was 100%, and precision was 100%.

Discussion

In this study, corneal biomechanical parameters were calculated using corneal dynamic deformation videos; this was achieved to distinguish keratoconus from normal corneas and has not been previously reported. We applied quantified corneal biomechanical properties in a 5-FNN model in the diagnosis of KC from a pure corneal biomechanical perspec-

Table 1. Comparative Results of Corneal Biomechanics

Characteristic	Sensitivity, %	Specificity, %
CRF	80.7	84.7
CH	85.5	89.1
5-FNN	99.3	100

CH, corneal hysteresis; CRF, corneal resistance factor.

Table 2. Model Comparison Results

Characteristic	Accuracy, %	Sensitivity, %	Specificity, %	Precision, %
CAD	98.4	97.1	99.6	99.6
SVM	96.9	92.8	98.2	94.6
5-FNN	99.6	99.3	100	100

CAD, computer-aided design; SVM, support vector machine.

tive without reliance on topography. The development of ML theory has provided new opportunities for the intelligent diagnosis of KC. A previous study using an automated decision tree achieved good diagnostic performance based on 55 morphologic features obtained by Pentacam.⁷ A computer-aided design model for the diagnosis of KC was constructed using 14 morphologic indices obtained by Pentacam with a sensitivity of 96.0% and a specificity of 99.3%.¹⁶ Meanwhile, another study used ML algorithms to construct a neural network model combining Pentacam and optical coherence tomography and captured 49 morphologic parameters for the diagnosis of early stage KC with a sensitivity and specificity of 98.5% and 94.7%, respectively.¹⁷ It is not hard to see that previous studies established intelligent diagnostic models of KC mostly based on corneal morphologic characteristics. However, in the early stages of KC, there are no obvious changes in corneal morphology, which means that there are no abnormalities on slit-lamp examination and corneal topography, and there are no obvious clinical signs of the disease. Roberts and Dupps¹⁸ suggested that the underlying cause of KC is an abnormality in the biomechanical properties of the cornea, while morphologic changes in the cornea are secondary manifestations. Based on this hypothesis, our study constructed an intelligent diagnostic model from the perspective of pure biomechanical properties to effectively distinguish KC from the normal cornea.

Corneal biomechanical properties show alterations in the early stages of KC,¹⁹ and corneal rigidity gradually declines with the progression of KC.²⁰ The keratoconus matching index and keratoconus matching probability provided by the Ocular Response Analyzer (Reichert Ophthalmic Instruments, Buffalo, NY, USA) were shown to be reliable indicators for the diagnosis of KC with an accuracy of 97.7%, sensitivity of 91.18%, and specificity of 94.34%.¹⁴ Sedaghat et al.¹¹ determined the role of corneal biomechanical properties and corneal morphologic characteristics in the detection of KC using linear regression models and found that certain parameters had good sensitivity and specificity for the diagnosis of KC. Another corneal biomechanical parameter, the Corneal Biomechanical Index, was introduced in 2016 to distinguish KC from normal eyes with a sensitivity of 94.1% and a specificity of 100%.²¹ Likewise, other studies reported good KC detection ability using corneal dynamic response parameters from the Corvis ST with linear regression models and random forests.^{13,15} It is noteworthy that these parameters are directly generated by the Ocular Response Analyzer or Corvis ST, and the dependency of the diagnostic model on the device may affect the general applicability of the model. Furthermore, it has also been demonstrated that, if there is a correlation

between parameters, both the accuracy and consistency of the model predictions are compromised.^{20,22} The 115,200 contour points on the cornea in our study were randomly selected for training. We used the traditional OTSU algorithm combined with morphology and logistics to extract corneal contours closer to the actual state based on the most original corneal dynamic deformation data to calculate parameters for true biomechanical properties at specific locations in the more adherent cornea. This allowed us to bring a new perspective on the diagnosis of KC from a biomechanical perspective.

Further analysis found that the correlation between the parameters we calculated was extremely weak; therefore, we did not need to account for the issue of limited model performance. We also investigated the role of corneal biomechanical parameters in the diagnosis of KC by visual analysis (Fig. 2). It was observed that the first A-time, HC-DA, and HC-R differed significantly between KC and normal corneas. The difference in CCT was not significant. However, previous studies have shown that CCT affects the biomechanical properties of the cornea.²³ Therefore, after evaluating the correlation and cumulative effects of these parameters, as well as the stability and repeatability of the measurements, we selected first A-time, HC-DA, HC-R, and CCT to train the 5-FNN model. At the same time, we recommend that these properties be used as typical KC diagnostic and screening indicators. In contrast to linear regression models, the 5-FNN model that our study uses is based on error backpropagation, which has a strong nonlinear fitting capability suitable for modeling complex nonlinear relationships. The 5-FNN model can fit any variable relationship with slightly better prediction accuracy. Furthermore, accuracy and sensitivity analyses of the model hyperparameters have been performed, and the advantages of the 5-FNN model are expected to increase as more corneal biomechanical features are incorporated into our training set.

The diagnosis of KC is currently based on clinical examination and corneal topography.²⁴ The biomechanical parameters described in our study provide a rationale for further quantitative analysis of KC diagnosis from a new perspective. It is a novel attempt, after which we will make gradual improvements, and the increased sample size for validation makes it more rigorous. A limitation of this study was its cross-sectional design. In future studies, we plan to also conduct fundamental research to explore the true biomechanical properties with the hope of achieving differentiation between the different severities of keratoconus. Furthermore, due to the complexity of viscoelastic biomechanical behavior as well as the influence of confounding factors, accurate assessment of

biomechanical properties in vivo is very difficult, and the real reaction in in vivo corneal biomechanics needs to be explored in the future.

In conclusion, this study enables automatic classification based solely on biomechanical parameters, calculated from pixel data during dynamic deformation of the cornea. This model provides a definitive diagnostic conclusion for KC from a purely corneal biomechanical perspective and demonstrates the feasibility and superiority of biomechanical properties in diagnosing KC. External validation was performed for the model's generalizability, and better validation results could be obtained with a larger sample data set. It is worth noting that this study analyzes corneal biomechanical properties using dynamic videos, but the acquisition of the videos is not limited to certain devices, meaning that our diagnostic model is valid as long as there is a video of corneal force deformation and interchangeable testing.

Acknowledgments

The authors thank all the participants who made this study possible and Editage (www.editage.cn) for English-language editing assistance.

Supported by the National Natural Science Foundation of China (No. 81873684).

Disclosure: **Z. Tan**, None; **X. Chen**, None; **K. Li**, None; **Y. Liu**, None; **H. Cao**, None; **J. Li**, None; **V. Jhanji**, None; **H. Zou**, None; **F. Liu**, None; **R. Wang**, None; **Y. Wang**, None

* ZT and XC contributed equally to this article.

References

- Rabinowitz YS. Keratoconus. *Surv Ophthalmol*. 1998;42(4):297–319.
- Ferrari G, Rama P. The keratoconus enigma: a review with emphasis on pathogenesis. *Ocul Surf*. 2020;18(3):363–373.
- Al-Amri AM. Prevalence of keratoconus in a refractive surgery population. *J Ophthalmol*. 2018;2018:5983530.
- Topol EJ. High-performance medicine: the convergence of human and artificial intelligence. *Nat Med*. 2019;25(1):44–56.
- Ting DSW, Pasquale LR, Peng L, et al. Artificial intelligence and deep learning in ophthalmology. *Br J Ophthalmol*. 2019;103(2):167–175.
- Lin SR, Ladas JG, Bahadur GG, Al-Hashimi S, Pineda R. A review of machine learning techniques for keratoconus detection and refractive surgery screening. *Semin Ophthalmol*. 2019;34(4):317–326.
- Smadja D, Touboul D, Cohen A, et al. Detection of subclinical keratoconus using an automated decision tree classification. *Am J Ophthalmol*. 2013;156(2):237–246.e1.
- Ruiz Hidalgo I, Rodriguez P, Rozema JJ, et al. Evaluation of a machine-learning classifier for keratoconus detection based on Scheimpflug tomography. *Cornea*. 2016;35(6):827–832.
- Arbelaez MC, Versaci F, Vestri G, Barboni P, Savini G. Use of a support vector machine for keratoconus and subclinical keratoconus detection by topographic and tomographic data. *Ophthalmology*. 2012;119(11):2231–2238.
- Salomão MQ, Hofling-Lima AL, Gomes Esporcatte LP, et al. The role of corneal biomechanics for the evaluation of ectasia patients. *Int J Environ Res Public Health*. 2020;17(6):E2113.
- Sedaghat MR, Momeni-Moghaddam H, Ambrósio R, et al. Diagnostic ability of corneal shape and biomechanical parameters for detecting frank keratoconus. *Cornea*. 2018;37(8):1025–1034.
- Liu Q, Gu Q, Wu Z. Feature selection method based on support vector machine and shape analysis for high-throughput medical data. *Comput Biol Med*. 2017;91:103–111.
- Elham R, Jafarzadehpur E, Hashemi H, et al. Keratoconus diagnosis using Corvis ST measured biomechanical parameters. *J Curr Ophthalmol*. 2017;29(3):175–181.
- Labiris G, Gatziofias Z, Sideroudi H, Giarmoukakis A, Kozobolis V, Seitz B. Biomechanical diagnosis of keratoconus: evaluation of the keratoconus match index and the keratoconus match probability. *Acta Ophthalmol*. 2013;91(4):e258–E262.
- Herber R, Pillunat LE, Raiskup F. Development of a classification system based on corneal biomechanical properties using artificial intelligence predicting keratoconus severity. *Eye Vis (Lond)*. 2021;8(1):21.
- Issarti I, Consejo A, Jiménez-García M, Hershko S, Koppen C, Rozema JJ. Computer aided diagnosis for suspect keratoconus detection. *Comput Biol Med*. 2019;109:33–42.
- Shi C, Wang M, Zhu T, et al. Machine learning helps improve diagnostic ability of subclinical keratoconus using Scheimpflug and OCT imaging modalities. *Eye Vis (Lond)*. 2020;7:48.
- Roberts CJ, Dupps WJ. Biomechanics of corneal ectasia and biomechanical treatments. *J Cataract Refract Surg*. 2014;40(6):991–998.

19. Shang J, Shen Y, Jhanji V, et al. Comparison of corneal biomechanics in Post-SMILE, Post-LASEK, and keratoconic eyes. *Front Med (Lausanne)*. 2021;8:695697.
20. Mikula E, Winkler M, Juhasz T, et al. Axial mechanical and structural characterization of keratoconus corneas. *Exp Eye Res*. 2018;175:14–19.
21. Vinciguerra R, Ambrósio R, Elsheikh A, et al. Detection of keratoconus with a new biomechanical index. *J Refract Surg*. 2016;32(12):803–810.
22. Nemeth G, Hassan Z, Csutak A, Szalai E, Berta A, Modis L. Repeatability of ocular biomechanical data measurements with a Scheimpflug-based non-contact device on normal corneas. *J Refract Surg*. 2013;29(8):558–563.
23. Herber R, Ramm L, Spoerl E, Raiskup F, Pillunat LE, Terai N. Assessment of corneal biomechanical parameters in healthy and keratoconic eyes using dynamic bidirectional applanation device and dynamic Scheimpflug analyzer. *J Cataract Refract Surg*. 2019;45(6):778–788.
24. Tian L, Ko MW, Wang LK, et al. Assessment of ocular biomechanics using dynamic ultra high-speed Scheimpflug imaging in keratoconic and normal eyes. *J Refract Surg*. 2014;30(11):785–791.